science, engineering and health studies

Research Article

Science, Engineering and Health Studies
https://lio1.tci-thaijo.org/index.php/sehs
ISSN (Online): 2630-0087

Simulation radiation shielding properties of tungsten carbide alloys

Sunantasak Ravangvong[1], Kittisak Sriwongsa[2], Pairoj Pasuwan[3], Punsak Glumglomchit[4], Priyakorn Khunnut[4], Panna Booncherttrong[4], and Isaravan Huekharnjiraroj[4]*

[1] Division of Science and Technology, Faculty of Science and Technology, Phetchaburi Rajabhat University, Phetchaburi 76000, Thailand
[2] Faculty of Education, Silpakorn University, Nakhon Pathom 73000, Thailand
[3] The Demonstration School of Silpakorn University, Nakhon Pathom 73000, Thailand
[4] Huahinvitthayalai School, Prachuap Khiri Khan 77000, Thailand

ABSTRACT

This work evaluated the gamma rays shielding properties of tungsten carbide alloys. The mass attenuation coefficients (μ_m) of gamma rays for these alloys have been obtained at gamma rays energy ranges of 356–1,332 keV using WinXCom software and FLUKA Monte Carlo code simulation. The results are found to be in good agreement. The 0.832W+0.0498C+0.002Co+0.00092Fe+0.107Ni alloy sample showed the highest μ_m and radiation protection efficiency (RPE%) values, while half value layer (HVL), mean free path (MFP) and transmission factor (TF%) values showed the lowest value compared with the others. These results indicate that this alloy sample, which has the highest density, possesses excellent γ-rays shielding properties.

Keywords: gamma rays shielding; mass attenuation coefficients; tungsten carbide alloys

***Corresponding author**:
Kittisak Sriwongsa
sriwongsa_k@silpakorn.edu

***Received**: 19 April 2024*
***Revised**: 13 December 2024*
***Accepted**: 22 February 2025*
***Published**: 19 November 2025*

***Citation**:
Ravangvong, S., Sriwongsa, K., Pasuwan, P., Glumglomchit, P., Khunnut, P., Booncherttrong, P., & Huekharnjiraroj, I. (2025). Simulation radiation shielding properties of tungsten carbide alloys. Science, Engineering and Health Studies, 19, 25020006.

1. INTRODUCTION

Lead is employed as a shielding material in a variety of radiation-related industries and other sectors. They are one of the most extensively utilized radiation shielding mediums for X-rays and gamma rays because of their high density (ρ), atomic number (Z), linear and mass attenuation coefficient (μ and μ_m) (Obaid et al., 2018; Manjunatha et al., 2017). However, ingesting or inhaling lead or lead-contaminated substances can be hazardous. After being exposed to lead at work, irradiation workers may bring lead residues and lead-exposed parts unknowingly back home (Mirji & Lobo, 2017; Kaur et al., 2019; Wani et al., 2015). Gamma rays are particularly harmful since they are uncharged and have a high-energy photon, resulting in an overpenetration that can harm human cells (Bushberg et al., 2012). The gamma rays could travel hundreds of meters through air and readily pass through the human body. The gamma rays attenuation is caused by its interaction with materials. The gamma rays attenuation capability is affected by incident gamma rays energy, atomic number, constituent density in the shielding material, and shielding material thickness (McAlister, 2012).

One of the most important elements to consider protecting people and the environment from the effects of radiation is the radiation attenuation capabilities of materials. Therefore, the radiation exposure to the operator in medical applications can be lowered to the lowest possible level by utilizing appropriate radiation shielding. High Z of elements are significant in radiation attenuation because the probability of photoelectric absorption to atoms within a material depends on the energy of the X-rays photon at impact and the atom's constituents of the irradiated body (Gavrish et al., 2016). As a result, the most appropriate form of attenuation is determined primarily by the cost, weight, chemical and physical durability of the material. Materials with a higher atomic number density are more attenuated than those with lower Z.

Toxic heavy metals, such as lead, have long-term negative impacts on health and the environment. As a result, several groups of radiation shielding scientists are interested in creating and researching non-toxic, lightweight, flexible, and low-cost shielding mediums to replace lead, which is desperately needed to replace lead shielding materials to attenuate radiation (AbuAlRoos et al., 2019). Lead-free materials, such as tungsten, are non-toxic; also, because of its higher atomic number, tungsten has a higher density and better masking capabilities than lead (Kobayashi et al., 1997). However, pure tungsten is relatively expensive, while having higher attenuation qualities and a lower half-value layer than standard lead shielding materials (Buyuk & Yugrul, 2014; Luković et al., 2015). The shielding capabilities of tungsten and epoxy composites were studied for low-energy gamma radiation at 122 keV (Chang et al., 2015), with the goal of evaluating the effectiveness of tungsten carbide as a shielding material for new lead-free radiation in nuclear medicine. The attenuation properties analysis results show that a high percentage of tungsten increases the radiation shielding properties of the samples.

The purpose of this research was to assess the performance of tungsten carbide alloys (WC-Fe, WC-Co, and WC-Ni) (Roulon et al., 2020) as lead-free radiation shielding alternatives in nuclear medicine. The FLUKA Monte Carlo code was used to simulate radiation transmission in the energy range of 356 to 1332 keV. The major characteristics to be investigated were the mass attenuation coefficients, half-value layer, mean free path, transmission factor, and radiation protection efficiency. The simulation results were compared with the theoretical values calculated by WinXCom software.

2. MATERIALS AND METHODS

2.1 Simulation setup and gamma rays interaction

The FLUKA is a Monte Carlo algorithm that was developed by CERN and INFN that includes a FLAIR interface for applications (Vlachoudis, 2009). This research was carried out using FLUKA version 4-3.3 under Fedora 37 (a Linux-based operating system), and the input file was edited with Flair version 3.2-4.5. The simulation computer system is an Intel Core i5-1235U with a 6.0 GHz CPU and 8 GB DDR4 RAM. To improve data dependability, the statistical error of the results to be less than 0.09% was chosen.

The FLUKA code was used to model the detector from Canberra Company. Previously, this detector was employed in similar experimental and modeling research (Shi et al., 2002; Tekin, 2016). The NaI(Tl) detector was used in this FLUKA simulation. The simulation of the NaI(Tl) scintillator detector can be referenced from previous research (Mouhti et al., 2017; Demir & Kuluöztürk, 2021). The relevant energy in the simulations is defined as isotropic gamma rays sources in the BEAM card (Ferrari et al., 2005). Figure 1 depicts the overall geometry of the successfully modeled NaI(Tl) detector.

The mass attenuation coefficients of the WC (Fe, Co, and Ni) were calculated at 356, 511, 662, 1173, 1275, and 1332 keV of gamma rays energies, which were also employed in absolute detector efficiency calculations. To simplify the mass attenuation coefficient (μ_m), it is necessary to understand the Lambert-Beer law, as illustrated in Eq. (1) (Sayyed et al., 2022):

$$I = I_0 e^{-\mu t} \quad (1)$$

where I_0 and I are the outputs of the USRTRACK scorecard without and with an absorber, respectively, μ is the linear attenuation coefficient, t denotes the absorber thickness, and I is the gamma rays intensity after passage through the absorber.

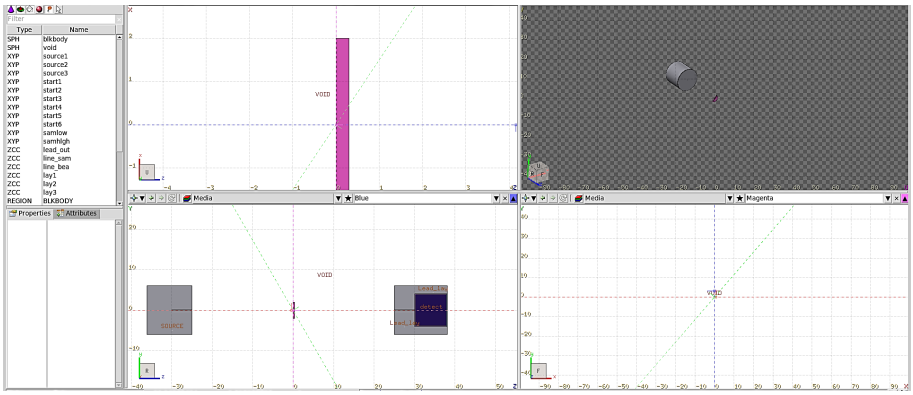

Figure 1. FLUKA code provided the schematic 2-D perspective and detailed coordinates of the simulated NaI(Tl) detector

The μ_m is μ divided by the density (ρ). It is commonly expressed in cm^2/g and can be calculated using the following Eq. (2) (Sayyed et al., 2022):

$$\mu_m = \frac{\mu}{\rho} \quad (2)$$

Half value layer (HVL) is defined as the thickness of alloys that decreases the gamma rays intensity to 50% of its initial intensity and was determined using μ by given in Eq. (3) (Sayyed et al., 2022; AbuAlRoos et al., 2020):

$$\text{HVL} = \frac{0.693}{\mu} \quad (3)$$

Mean free path (MFP) is the average distance between two successive interactions of gamma rays in alloys and is evaluated from Eq. (4) (Sayyed et al., 2022; AbuAlRoos et al., 2020):

$$\text{MFP} = \frac{1}{\mu} \quad (4)$$

The transmission factor (TF) is a value used to predict the coefficient of gamma rays transport through a thickness of alloys as can be calculated using the Eq. (5) (Sayyed et al., 2022; Hanfi et al., 2023):

$$\text{TF} = \frac{I}{I_o} \times 100 = e^{-\mu x} \quad (5)$$

where x is sample thickness.

The radiation protection efficiency (RPE) can be determined using Eq. (6) (Hanfi et al., 2023):

$$\text{RPE} = \left(1 - \frac{I}{I_0}\right) \times 100\% \quad (6)$$

2.2 Alloys description

The chemical composition for tungsten carbide alloys: WC (Fe, Co, and Ni) alloy samples is displayed in Table 1.

Table 1. Chemical composition for tungsten carbide alloys (% w/w) (Roulon et al., 2020)

Alloy code	Chemical composition (% w/w)				
	W	C	Co	Fe	Ni
S1	0.8290	0.0555	0.0021	0.1100	0.0034
S2	0.8320	0.0530	0.0021	0.1095	0.0034
S3	0.8200	0.0593	0.0020	0.1158	0.0029
S4	0.8230	0.0525	0.0027	0.0009	0.1127
S5	0.8320	0.0498	0.0020	0.0009	0.1070
S6	0.8210	0.0549	0.0020	0.0006	0.1160

3. RESULTS AND DISCUSSION

The density of tungsten carbide alloys was exhibited as shown in Figure 2. It was found that the density of the S5 alloy sample had the highest value. This event is due to the S5 alloy sample having high W and Ni content (Sriwongsa et al., 2023).

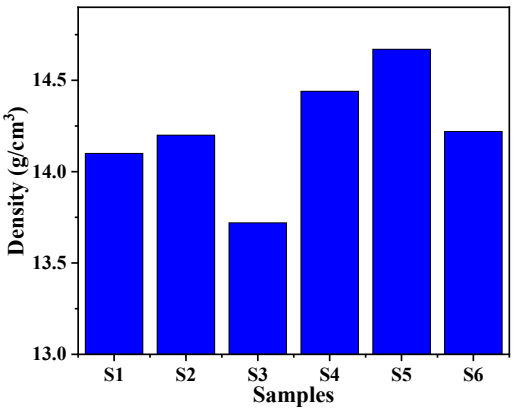

Figure 2. Density of tungsten carbide alloys

The mass attenuation coefficient (μ_m) for tungsten carbide alloys at gamma rays energy ranges from 356–1332 keV at thicknesses of 0.1–0.3 cm, as exhibited in Figure 3. The sources of gamma rays were ^{22}Na (511 and 1275 keV), ^{133}Ba (356 keV), ^{137}Cs (662 keV), and ^{60}Co (1173 and 1332 keV) for the transmission event. It was found that the results from WinXCom software and FLUKA Monte Carlo code simulation are in good agreement. In addition, it was found that the μ_m values decreased with increasing the gamma rays energy. It is according to the major photoelectric effect (PE) process at low energy ranges where the PE probability is large (Sriwongsa et al., 2023).

The HVL and MFP values at gamma rays energy ranging from 356–1332 keV were displayed in Figures 4 and 5. It was found that these values increased with increasing gamma rays energy, and the S5 alloy sample shown the lowest value. It indicated that high density would be superb gamma rays shielding (Sriwongsa et al., 2023).

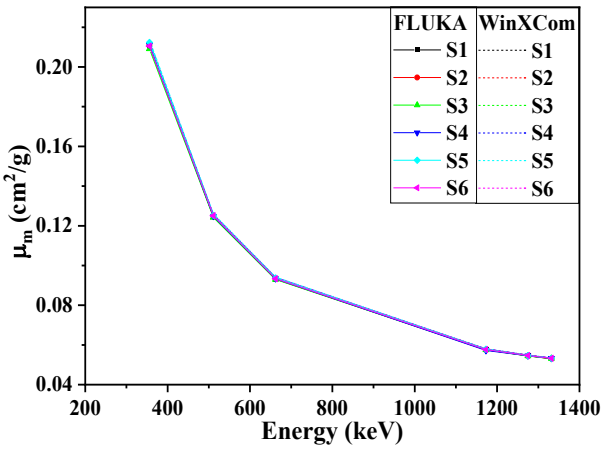

Figure 3. Mass attenuation coefficient for alloys at gamma rays energy range of 356–1332 keV

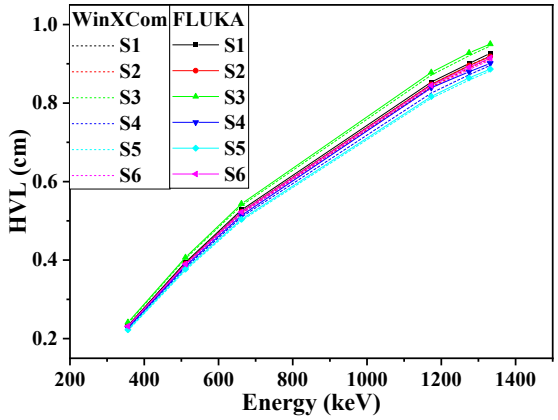

Figure 4. HVL for alloys at gamma rays energy range of 356–1332 keV

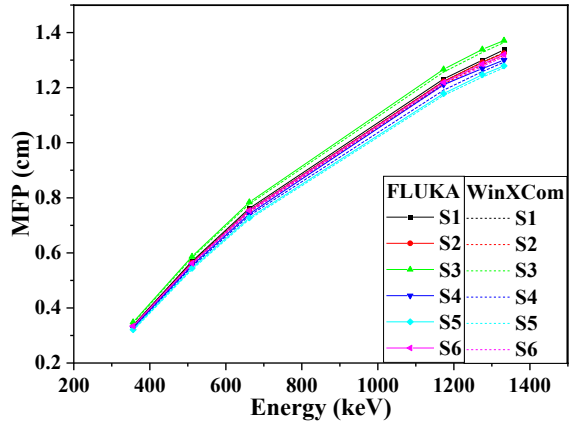

Figure 5. MFP for alloys at gamma rays energy range of 356–1332 keV

TF of alloys with gamma rays energy is shown in Figure 6. TF values increased with increasing gamma rays energy and S5 alloy sample has the lowest TF value at the same gamma rays energy. It indicated that the S5 sample exhibited good transmission value shielding powerful gamma rays (Tekin et al., 2022).

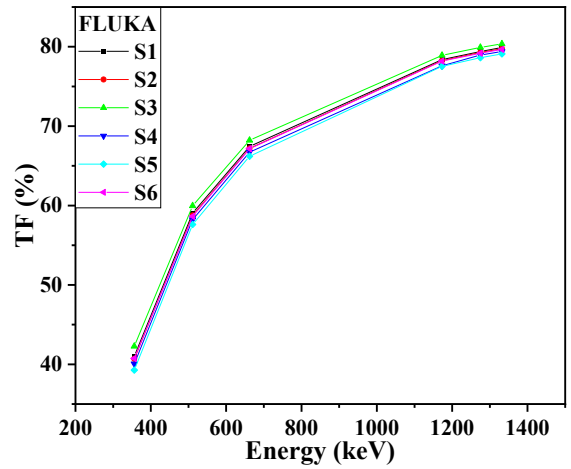

Figure 6. Transmission factor (TF) for alloys at gamma rays energy range of 356–1332 keV

The RPE for alloys is shown in Figure 7. It was found that the S5 alloy sample has the maximum RPE value. It indicated the excellent shielding performance of the S5 alloy sample. Also, from Figure 7, more gamma rays are being transmitted with increased energy. So, to improve the shielding properties, it can be done by increasing the thickness of the alloy (Sayyed et al., 2019).

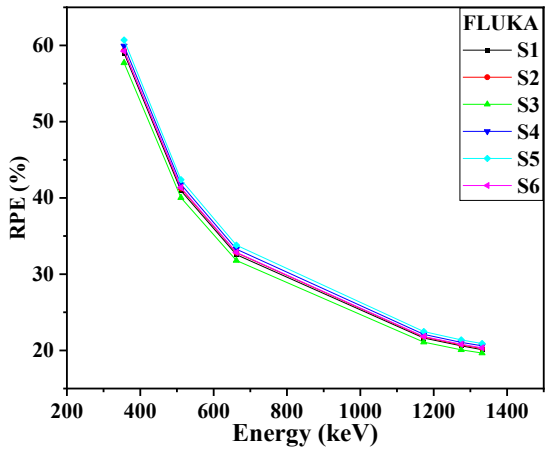

Figure 7. Radiation protection efficiency (RPE) for alloys at gamma rays energy range of 356–1332 keV

4. CONCLUSION

From the available results of the study, shielding properties for gamma rays of the tungsten carbide alloys, including the μ_m, HVL, MFP, TF, and RPE values were discussed at energies range of 356–1332 keV using the FLUKA Monte Carlo code simulation and compared with WinXCom software. The simulation results were in a good agreement with theoretical data. In addition, the 0.832W+0.0498C+0.002Co+0.00092Fe+0.107Ni alloy sample, which had the largest density, has the highest μ_m and RPE, while HVL, MFP, and TF showed the lowest values. These results indicated that gamma rays shielding properties depended on the density of the alloy.

ACKNOWLEDGMENTS

This research is financially supported by Thailand Science Research and Innovation (TSRI) National Science, Research and Innovation Fund (NSRF) (Fiscal Year 2023).

REFERENCES

AbuAlRoos, N. J., Amin, N. A. B., & Zaino, R. (2019). Conventional and new lead-free radiation shielding materials for radiation protection in nuclear medicine: A review. *Radiation Physics and Chemistry*, *165*, Article 108439. https://doi.org/10.1016/j.radphyschem.2019.108439

AbuAlRoos, N. J., Azman, M. N., Amin, N. A. B., & Zainon, R. (2020). Tungsten-based material as promising new lead-free gamma radiation shielding material in nuclear medicine. *Physica Medica*, *78*, 48–57. https://doi.org/10.1016/j.ejmp.2020.08.017

Bushberg, J. T., Seibert, J. A., Leidholdt, E. M., Jr., & Boone, J. M. (2012). *The essential physics of medical imaging* (3rd ed.). Wolters Kluwer.

Buyuk, B., & Yugrul, A. B. (2014). Comparison of lead and WC-Co materials against gamma irradiation. *Acta Physica Polonica Series A*, *125*(2), 423–425. http://doi.org/10.12693/APhysPolA.125.423

Chang, L., Zhang, Y., Liu, Y., Fang, J., Luan, W., Yang, X., & Zhang, W. (2015). Preparation and characterization of tungsten/epoxy composites for γ-rays radiation shielding. *Nuclear Instruments and Methods in Physics Research Section B: Beam Interactions with Materials and Atoms*, *356–357*, 88–93. https://doi.org/10.1016/j.nimb.2015.04.062

Demir, N., & Kuluöztürk, Z. N. (2021). Determination of energy resolution for a NaI(Tl) detector modeled with FLUKA code. *Nuclear Engineering and Technology*, *53*(11), 3759–3763. https://doi.org/10.1016/j.net.2021.05.017

Ferrari, A., Sala, P. R., Fasso, A., & Ranft, J. (2005). *FLUKA: A multi-particle transport code* (CERN-2005-010; SLAC-R-773; INFN-TC-05-11). European Organization for Nuclear Research (CERN).

Gavrish, V. M., Baranov, G. A., Chayka, T. V., Derbasova, N. M., Lvov, A. V., & Matsuk, Y. M. (2016). Tungsten nanoparticles influence on radiation protection properties of polymers. *IOP Conference Series: Materials Science and Engineering*, *110*, Article 012028. https://doi.org/10.1088/1757-899X/110/1/012028

Hanfi, M. Y., Sakr, A. K., Ismail, A. M., Atia, B. M., Alqahtani, M. S., & Mahmoud, K. A. (2023). Physical characterization and radiation shielding features of B_2O_3-As_2O_3 glass ceramic. *Nuclear Engineering and Technology*, *55*(1), 278–284. https://doi.org/10.1016/j.net.2022.09.006

Kaur, T., Sharma, J., & Singh, T. (2019). Review on scope of metallic alloys in gamma rays shield designing. *Progress in Nuclear Energy*, *113*, 95–113. https://doi.org/10.1016/j.pnucene.2019.01.016

Kobayashi, S., Hosoda, N., & Takashima, R. (1997). Tungsten alloys as radiation protection materials. *Nuclear Instruments and Methods in Physics Research Section A: Accelerators, Spectrometers, Detectors and Associated Equipment*, *390*(3), 426–430. https://doi.org/10.1016/S0168-9002(97)00392-6

Luković, J., Babić, B., Bučevac, D., Prekajski, M., Pantić, J., Baščarević, Z., & Matović, B. (2015). Synthesis and characterization of tungsten carbide fine powders. *Ceramics International*, *41*(1 Part B), 1271–1277. https://doi.org/10.1016/j.ceramint.2014.09.057

Manjunatha, H. C., Seenappa, L., Chandrika, B. M., & Hanumantharayappa, C. (2017). A study of photon interaction parameters in barium compounds. *Annals of Nuclear Energy*, *109*, 310–317. https://doi.org/10.1016/j.anucene.2017.05.042

McAlister, D. R. (2012). *Gamma ray attenuation properties of common shielding materials*. University Lane.

Mirji, R., & Lobo, B. (2017). Radiation shielding materials: A brief review on methods, scope and significance. In *Proceedings of the National Conference on 'Advances in VLSI and Microelectronics'* (pp. 96–100). P.C. Jabin Science College.

Mouhti, I., Elanique, A., & Messous, M. Y. (2017). Monte Carlo modelling of a NaI(Tl) scintillator detectors using MCNP simulation code. *Journal of Materials and Environmental Sciences*, *8*(12), 4560–4565. https://doi.org/10.26872/jmes.2017.8.12.481

Obaid, S. S., Gaikwad, D. K., & Pawar, P. P. (2018). Determination of gamma ray shielding parameters of rocks and concrete. *Radiation Physics and Chemistry*, *144*, 356–360. https://doi.org/10.1016/j.radphyschem.2017.09.022

Roulon, Z., Missiaen, J. M., & Lay, S. (2020). Carbide grain growth in cemented carbides sintered with alternative binders. *International Journal of Refractory Metals and Hard Materials*, *86*, Article 105088. https://doi.org/10.1016/j.ijrmhm.2019.105088

Sayyed, M. I., Akman, F., Kaçal, M. R., & Kumar, A. (2019). Radiation protective qualities of some selected lead and bismuth salts in the wide gamma energy region. *Nuclear Engineering and Technology*, *51*(3), 860–866. https://doi.org/10.1016/j.net.2018.12.018

Sayyed, M. I., Dwaikat, N., Mhareb, M. H. A., D'Souza, A. N., Almousa, N., Alajerami, Y. S. M., Almasoud, F., Naseer, K. A., Kamath, S. D., Khandaker, M. U., Osman, H., & Alamri, S. (2022). Effect of TeO_2 addition on the gamma radiation shielding competence and mechanical properties of boro-tellurite glass: An experimental approach. *Journal of Materials Research and Technology*, *18*, 1017–1027. https://doi.org/10.1016/j.jmrt.2022.02.130

Shi, H.-X., Chen, B.-X., Li, T.-Z., & Yun, D. (2002). Precise Monte Carlo simulation of gamma-ray response functions for an NaI(Tl) detector. *Applied Radiation and Isotopes*, *57*(4), 517–524. https://doi.org/10.1016/S0969-8043(02)00140-9

Sriwongsa, K., Tantiamnuay, P., Thepchai, P., Glumglomchit, P., Papatron, P., Yangyuen, P., Ravangvong, S., Khobkham, C., Mutuwong, C., & Bootjomchai, C. (2023). The Gamma Ray, thermal and fast neutrons shielding properties of Gd_2O_3-SiO_2-Y_2O_3-CaO-B_2O_3 glass series using FLUKA simulation code. *Science Essence Journal*, *39*(1), 27–40. https://ejournals.swu.ac.th/index.php/sej/article/view/14948

Tekin, H. O. (2016). MCNP-X Monte Carlo code application for mass attenuation coefficients of concrete at different energies by modeling 3 x 3 inch NaI(Tl) detector and comparison with XCOM and Monte Carlo data. *Science and Technology of Nuclear Installations*, *2016*(1), Article 6547318. https://doi.org/10.1155/2016/6547318

Tekin, H. O., ALMisned, G., Rammah, Y. S., Ahmed, E. M., Ali, F. T., Baykal, D. S., Elshami, W., Zakaly, H. M. H., Issa, S. A. M., Kilic, G., & Ene, A. (2022). Transmission factors, mechanical, and gamma ray attenuation properties of barium-phosphate-tungsten glasses: Incorporation impact of WO_3. *Optik*, *267*, Article 169643. https://doi.org/10.1016/j.ijleo.2022.169643

Vlachoudis, V. (2009). Flair: A powerful but user friendly graphical interface for FLUKA. In *International Conference on Mathematics, Computational Methods & Reactor Physics 2009* (pp. 790–800). American Nuclear Society. https://cds.cern.ch/record/2749540/?ln=en

Wani, A. L., Ara, A., & Usmani, J. A. (2015). Lead toxicity: A review. *Interdisciplinary Toxicology*, *8*(2), 55–64. https://doi.org/10.1515/intox-2015-0009